Electrochimica Acta 283 (2018) 1384–1389

Contents lists available at ScienceDirect

Electrochimica Acta

journal homepage: www.elsevier.com/locate/electacta

Facile solid-state synthesis of eco-friendly sodium iron silicate with exceptional sodium storage behaviour

Karthikeyan Kaliyappan**, Zhongwei Chen*

Department of Chemical Engineering, University of Waterloo, 200 University Avenue West, Waterloo, Ontario N2L 3G1, Canada

ARTICLE INFO

Article history:
Received 7 April 2018
Received in revised form
25 June 2018
Accepted 8 July 2018
Available online 10 July 2018

Keywords:
Na_2FeSiO_4
Sodium ion batteries
Solid state
High rate performance
Polyanion cathode

ABSTRACT

It is crucial to develop stable energy sources for rechargeable sodium-ion batteries using simple synthesis methods. Herein, we report a facile route for synthesizing phase-pure carbon-coated Na_2FeSiO_4 polyanionic cathodes using conventional solid-state methods at 700 °C under inert atmosphere. X-ray diffraction results reveal that there are no impurities in the highly crystalline Na_2FeSiO_4 particles, resulting from the heat of combustion provided by the organic chelating agent. The electrochemical behaviour of Na_2FeSiO_4 particles is tested within 1.5–4.5 V at 0.25 C. The Na_2FeSiO_4 cathode delivered 119 mAh g^{-1} at 0.25 C and maintained ~85% of its initial capacity after 200 cycles after activation process. Even at high current densities of 3.5 C, the material outperforms other orthosilicates-based cathodes reported with capacities of 55 mAh g^{-1} discharge capacity along with ~80% retention after 1000 cycles. The enhanced performance of carbon-coated Na_2FeSiO_4 particles is ascribed to the improved electronic conductivity by the incorporation of carbon and the presence of void space between the particles. This void space contains more electrolytes and eliminates the stress formed during the cycling process, thus improving stability even at high rates. This is the first report on obtaining phase pure metal orthosilicate material with negligible impurities using simple solid-state method along with such exponential electrochemical performances.

1. Introduction

Many studies have been devoted to the design of next-generation energy storage devices that are low-cost and environmentally benign due to the vast commercialization of portable electronic devices and increasing awareness of global warming [1]. Although lithium-sulfur and metal-air batteries are considered as promising alternatives to lithium-ion batteries (LIBs), their complex storage mechanisms make them inappropriate for commercial applications [2,3]. Sodium-based rechargeable batteries (RSBs) can provide significant advantages, including large availability of sodium resources and low toxicity, which make them a better candidate to replace LIBs [4]. The first work on the RSB was reported in the 1970s [5,6]. Due to the massive commercialization of LIB cells in the early 1990s, research focusing on sodium-based chemistry had significantly reduced. Recently, numerous works demonstrated high-performance cathode materials for RSBs to replace toxic LIBs [2,4,7,8]. Specifically, focus is being made to develop p2-type layered materials due to its high capacity and facile synthesis [2,7,9,10]. However, severe capacity decay at high voltage operation occurs due to phase transition, and this hinders its potential utilization in next-generation RSBs [9–11].

On the other hand, with polyanionic compounds such as olivine, NASICON materials are known to exhibit stable electrochemical performance at lower operating voltages [12–14]. Although these materials displayed excellent cyclic stability, low cut-off voltages and complicated synthesis processes make them unsuitable for large-scale application. Recently, sodium orthosilicates (Na_2MSiO_4, M = Fe and Mn) have attracted a great amount of attention as a result of their high theoretical capacity (>270 mAh g^{-1} when extracting two Na^+ ions per formula unit) and high thermal stability through strong Si–O bonding [15,16]. In addition, the high availability of earth-abundant materials such as Fe and Si can help to make Na_2FeSiO_4 (NFSO) the cheapest energy source available for RSBs [17]. However, NFSO still requires a great deal of attention to enhance its electrochemical performance. Zhang et al. initially prepared NFS from Li_2FeSiO_4 (LFS) using a complex electrochemical

* Corresponding author.
** Corresponding author.
E-mail addresses: karthik506@gmail.com (K. Kaliyappan), zhwchen@uwaterloo.ca (Z. Chen).

https://doi.org/10.1016/j.electacta.2018.07.034
0013-4686/

ion-exchange (EIE) method and reported two Na-ion extractions from the NFS structure with a discharge capacity of 330 mAh g^{-1} [18]. Later, many studies demonstrated the design of carbon-coated NFS (NFSO-C) using solution-based synthesis methods [16,19–22].

However, most of them are reported with impurity phases, which is not beneficial for long term cycling as well as rate performance [16,21,23]. In addition, their synthesis methods hydrothermal (HT) or spray drying (SD) or sol-gel (SG) methods) are also contained complicated steps and required prolonged time to get the final product. For instance, Kee et al. reported the preparation NFSO-C using HT at 230 °C for 7 days followed by high temperature drying at 300 °C for two days [16]. On the other hand, SG synthesis of NFS required ex-situ carbon-coating using sucrose as a carbon source and displayed poor capacity retention after 100 cycles [16,19–23]. The EIE/SG/HT synthesis of NFSO reported thus far includes complicated multi-step preparation techniques and fails to control surface morphology, which leads to severe aggregation of NFSO [16,21]. This can, in turn, reduce the electrochemical performance of the electrode due to the poor optimization of these synthesis techniques [16,24,25]. Most of the studies which synthesize NFSO-C using SG or HT techniques involve ball milling to coat carbon [16,25]. Thus, a simple and facile synthesis route is vital to develop highly pure NFSO-C cathodes with better cycling and rate capabilities.

It is well known that the solid-state (SS) route is an appropriate method to prepare polycrystalline materials for mass production on the industrial scale. Herein, we report the synthesis of in-situ carbon-coated, highly crystalline NFSO cathodes with negligible impurity phases by a conventional one-step SS method using adipic acid (AA) as the carbon source. The potential application of NFSO-C in RSBs is tested at different current densities between 1.5 V and 4.5 V at room temperature. The NFSO-C displays high crystallinity along with enhanced electrochemical stability for prolonged cycling when compared to NFSO-C prepared using SG or HT methods. This result certainly provides the possibility of adopting Fe-based cathode materials in next-generation batteries to drive zero emission vehicles in the near future.

2. Experimental

High pure carbon-coated NFSO (NFSO-C) nanoparticles are synthesized using analytical grade $Na_2C_2O_4$ (Sigma-Aldrich, USA), FeC_2O_4 (Sigma-Aldrich, USA) $C_6H_{10}O_4$ (Sigma-Aldrich, USA) and fumed SiO_2 (Sigma-Aldrich, USA) using a single-step conventional solid-state method. Adipic acid ($C_6H_{10}O_4$, Aldrich, USA, 99%) is used as the carbon source and chelating agent to suppress particle agglomeration during the synthesis, and its concentration was fixed at 1 M. Stoichiometric amounts of the starting materials are mixed well using a mortar and pestle along with the chelating agent for 30 min. Finally, this mixture is fired at 700 °C for 12 h under Ar flow to get the resulting NFSO-C powder.

The crystalline nature of the as-prepared NFSO-C is examined using powder X-ray diffraction (XRD, Miniflex 600, Rigaku, Japan) measurements with Cu-Ka as the radiation source. The morphological features of the nanoparticles recaptured using a high-resolution scanning electron microscope (HR-SEM, LEO Zeiss 1550, Switzerland) and transition electron microscope (HR-TEM, JEOL 2010 FEG). The valence state of the metal ions is determined using X-ray photoelectron spectroscopy (XPS, Thermo Scientific Theta Probe, USA). Thermogravimetric analysis (TGA, TA instrument Q500) is performed to measure the amount of carbon present in the NFSO-C sample. The active Brunauer-Emmett-Teller (BET) surface area of NFSO-C is measured using a Micromeritics ASAP 2020 surface area analyzer. Electrochemical measurements of the NFSO-C cathode are conducted in a CR 2032 cell configuration in which the NFSO-C slurry is pressed on a stainless steel mesh in which NFSO-C serves as the cathode, and metallic Na foil acts as the anode. The detailed preparation of the NFSO-C slurry was carried out according to our previous work [26,27]. Charge-discharge (C/DC) studies of NFSO-C are conducted between 1.5 V and 4.5 V at different current rates (using 1 C = 140 mAh g^{-1}). Electrochemical impedance spectra (EIS, Bio-logic, DSP-300, France) are recorded before and after cycling at different current rates. Spectra are recorded between 200 kHz and 100 MHz.

3. Results and discussion

The crystalline nature of the NFSO-C examined though XRD is presented in Fig. 1a. The XRD of NFSO-C can be indexed to the Na_2ZnSiO_4 phase with the P1n1 (SG:7) space group according to the ICSD card number #18314, which is in accordance with recent reports on Na_2MnSiO_4 [15,16,23]. As seen in Fig. 1a, the XRD peaks are sharp with no peaks corresponding to major impurity phases such as Na_2SiO_3 and Fe_3O_4, demonstrating the formation of phase-pure, highly crystalline NFSO-C nanoparticles. The insertion in Fig. 1a displays the magnified XRD pattern of NFSO-C, which further confirms that there are no unindexed peaks in the pattern. The lattice cell contents of NFSO-C are calculated as a = 7.129 Å, b = 5.581 Å, and c = 5.473 Å from the XRD patterns. These lattice parameter values are in well agreement with the previous reports on NFSO [16]. It is noteworthy that this is the first report on synthesizing metal orthosilicates with negligible impurity phases compared to the work reported elsewhere [15,16,19–23,25]. In addition, the NFSO-C exhibits a BET surface area of 5 m^2 g^{-1}, which is relatively high for a material prepared from conventional SS method.[16,19,22] The reason for the formation of highly crystalline NFSO-C nanoparticles along with high active surface area even at low calcination temperature of 700 °C can be explained as follows: The addition of carboxylic acid during the synthesis as a chelating agent not only prevents the aggregation of NFS particles but also provides the required heat of combustion to synthesis highly crystalline NFSO-C powders [24,28]. In turn, the particles became fluffy and swelled greatly when the calcination temperature reached 400 °C due to the formation of void spaces by the evolution of carbon oxides (CO and CO_2) during the decomposition of carboxylic acid [28]. Consequently, the higher heat of combustion can naturally lead to highly crystalline NFSO-C with a high surface area. The carbon content in NFSO-C is calculated to be approximately 5% using TGA analysis.

The SEM images of NFSO-C in Fig. 1b provide further evidence of this phenomenon, clearly showing the presence of void space on the surface of the particles, which can be formed through CO and CO_2 evolution [28]. As seen from the SEM images, the NFSO-C exhibited composite texture with highly interconnected primary particles with an average size of about ~110 nm and an evenly sized distribution. The chelating agent added in the preparation shortens the Na-Fe-Si distance and enhances the crystallization between the cations as well as the homogeneity of the final product [24,26,28]. Subsequently, the evenly sized particles shorten the pathway for ionic diffusion and the void space on the surface stores more electrolytes within its structure as confirmed by SEM analysis. The former enhances the conductive nature of the materials and the latter reduces the inherent mechanical stress during the C/DC cycles [29]. Both morphological features assist to improve the electrochemical stability and rate performance of the cathode.

The TEM image of NFSO-C is presented in Fig. 1c and the corresponding high magnification image is shown as the insert. HR-TEM images shown in the insertion of Fig. 1c demonstrates the presence of a uniform layer of carbon (~2–3 nm) and hollow spaces on NFSO particles. As seen from the TEM image, the aggregated

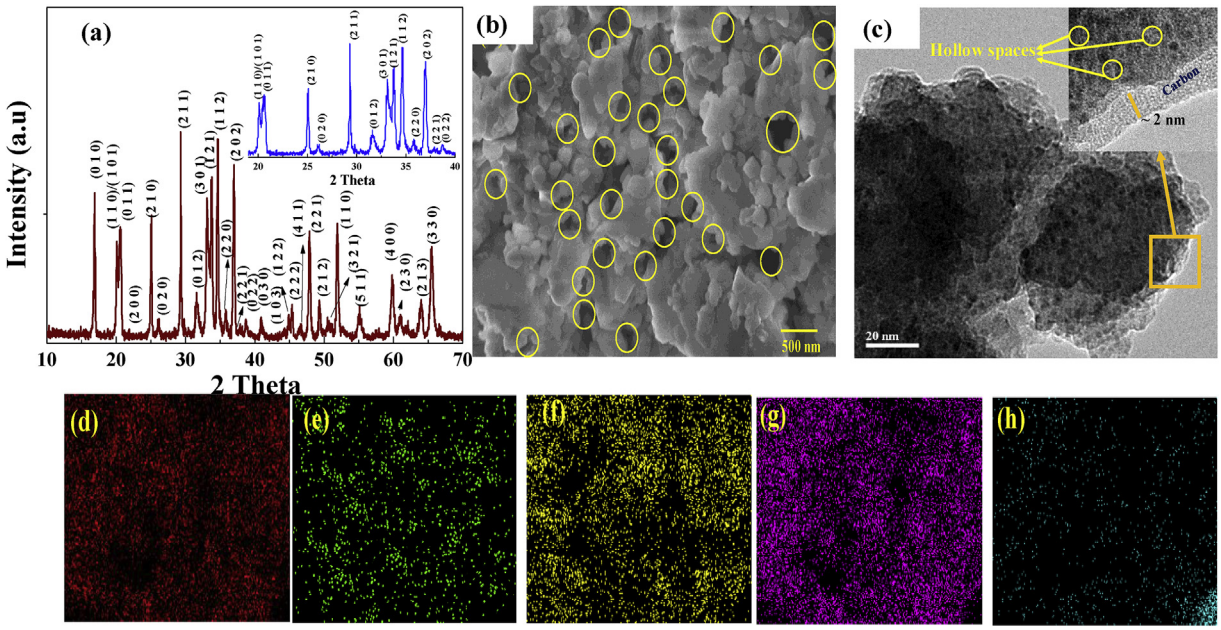

Fig. 1. (a) XRD and (d) SEM and (c) TEM of NFSO-C prepared using conventional SS method at 700 °C for 12 h. Elemental mapping of (d) Na, (e) Si (f) Fe, (g) O and (h) C distribution. Insert in figure (a) presents the zoomed area of XRD of NFSO-C.

NFSO-C secondary particles are composed of primary nanoparticles with an average size of 100–150 nm with a porous structure. It is well known that the formation of the porous structure originates from the decomposition of organic agents and subsequent release of gas [30]. This porous structure allows the electrolyte to access every NFSO grain, making Na^+ intercalation/deintercalation (I/DI) easier between electrolyte and NFSO-C particles [31]. Moreover, these closely packed particles with carbon coating further enhances the electronic conductivity of the cathode materials [15]. In addition, the metallic distribution of NFSO-C particles is examined using EDX analysis and their corresponding mapping is presented in Fig. 1d–h. The EDX elemental mappings of Na, Si, Fe, O and C in Fig. 1 confirm the atomic level distribution of starting materials.

The XPS spectrum in Fig. 2a discloses the presence of C 1s, Na 1s, Fe 2p, Si 2s, Si 2p, and O 1s in NFSO-C. The high-resolution XPS of Fe 2p is presented in Fig. 2b, which contains two parts (Fe $2p_{3/3}$ and Fe $2p_{1/2}$) due to spin-orbit coupling [32]. The binding energy at 710. 1 and 725.5 eV can be attributed to Fe $2p_{3/2}$ and Fe $2p_{1/2}$, respectively, which are the typical characteristic of the presence of ferric at the surface of the NFSO-C sample [30,32]. The presence of ferric on the NFSO-C samples is probably resulting from surface oxidation after etching with the argon ion during the calcination process. It is worth mentioning here that there is no satellite peak of y-Fe_3O_4 as noted at 719 eV, further validating that the electrode material is void of impurities and that the starting material did not decompose to y-Fe_3O_4 [32,33]. This confirms that there is no formation of the non-conductive magnetite phase in NFSO-C that can affect electrochemical performance, which is also confirmed by the XRD. The Na 1s spectrum (Fig. 2c) presents a peak centred at 1072.1 eV, demonstrating an oxidation state +1. The XPS spectrum of Si 2p (Fig. 2d) and O 1s (Fig. 2e) have corresponding peaks at 531.5 eV and 101.9 eV, respectively [34]. The de-convoluted C 1s spectrum in Fig. 2f exhibits characteristic peaks at 283.5 eV, 285.4 eV, 286.6 eV, 288.2 eV, and 289.3 eV, which are assigned to the sp^2 carbon, C-OH, epoxy, C=O, and π-π* functionalities, respectively [31,32]. These small oxygen-containing functionalities are crucial to ensure long-term electrochemical cycling [35]. This is due to the fact that the presence of higher surface oxygen functionalities affects the electrical conductivity profile and is involved in an unwanted side reaction with the electrolyte counterpart [32,35].

The C/DC profile of NFSO-C electrode vs Na metal foil in 1 M $NaClO_4$ dissolved in ethyl carbonate: diethyl carbonate (DEC) (1:1, v/v) is illustrated in Fig. 3a. The C/DC characteristics are recorded between 1.5 V and 4.5 V at 0.25 C. The half cell is initially tested at 0.25 C for five cycles to activate/stabilize the electrode-electrolyte interfacial layer (SEI) for long-term cycling. The NFSO-C/Na^+ cell delivered an initial charge and discharge capacities of 260 and 120 mAh g^{-1}, respectively, at a current rate of 0.25 C. This corresponds to the extraction of 1.91 M of sodium from NFSO-C structure during the charging process and the reinsertion of 0.9 M Na-ions into its structure during the discharging, resulting in an initial coulombic efficiency (CE) of approximately 50%. However, the CE increases to ~90% after this activation step (Fig. 3b). It is well known that the large irreversible capacity loss is normal for polyanion-based materials, being attributed to electrolyte decomposition, possible irreversible electrode reduction, and inevitable SEI formation [19,20,34]. There are two voltage plateaus observed in Fig. 3a at 2.0 V and 4.3 V in the C/DC profile, confirming a multi-step electrochemical reaction as reported elsewhere [19,25].

After the activation step, the NFSO-C/Na^+ cell exhibits a discharge capacity of 105 mAh g^{-1} at 0.25 C. The discharge capacities realized from the NFSO-C/Na^+ cell surpasses many reported values on NFSO. For instance, NFSO prepared using HT and SG methods exhibit discharge capacities of 86 and 105 mAh g^{-1} at the current rate of C/20 and C/15, respectively along with severe capacity decay [16,21]. NFSO synthesized using HT method shows roughly 40% of cyclic stability after 20 cycles [16,21]. Recently, other orthosilicates materials (Na_2MSiO_4 where M = Co or Mn) also report to deliver slightly enhanced discharge capacity values [15,36–38]. However, these studies utilize either large quantities of graphene (>25 wt %) or high-cost electrolyte (ionic liquids or vinyl carbonate additives) to improve its electrochemical performance, which is not appropriate for practical applications [15,36–38]. In contrast, this work succeeds in demonstrating the development of sodium orthosilicates using a simple solid-state method with superior electrochemical performance when compared to solution-

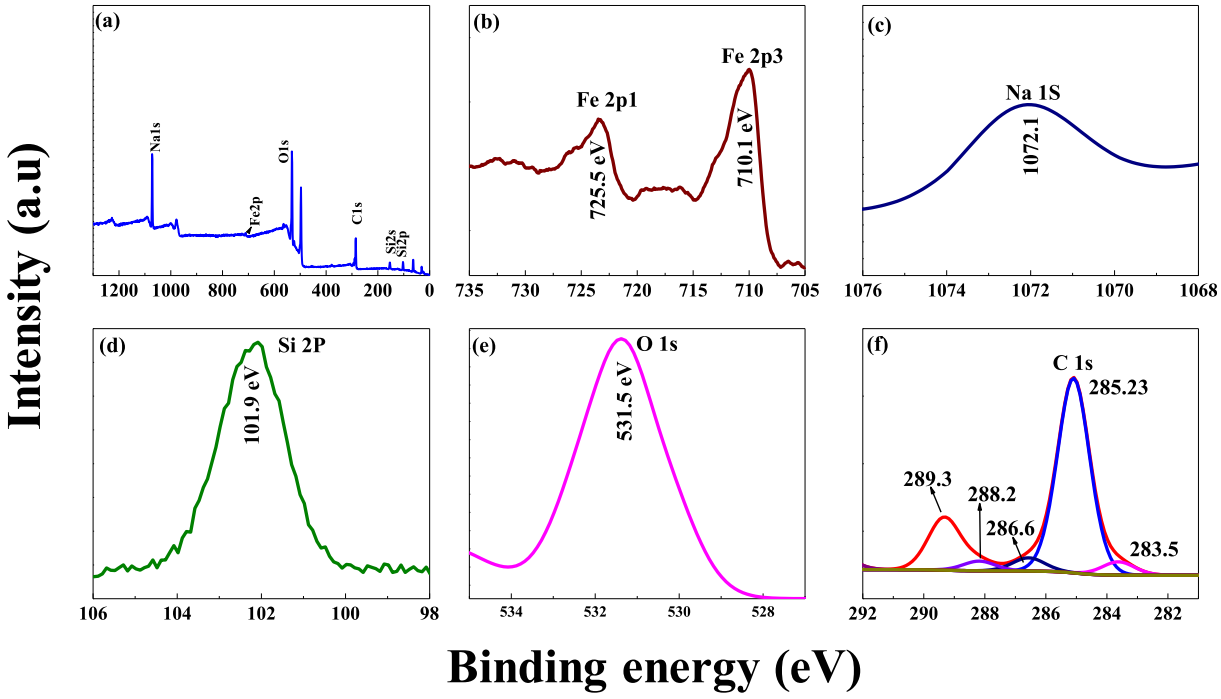

Fig. 2. XPS spectrums of (a) NFSO-C prepared by solid state method (b) Fe 2p, (c) Na 1s, (e) Si 2p, (f) O 1s, and (e) C 1s spectrum.

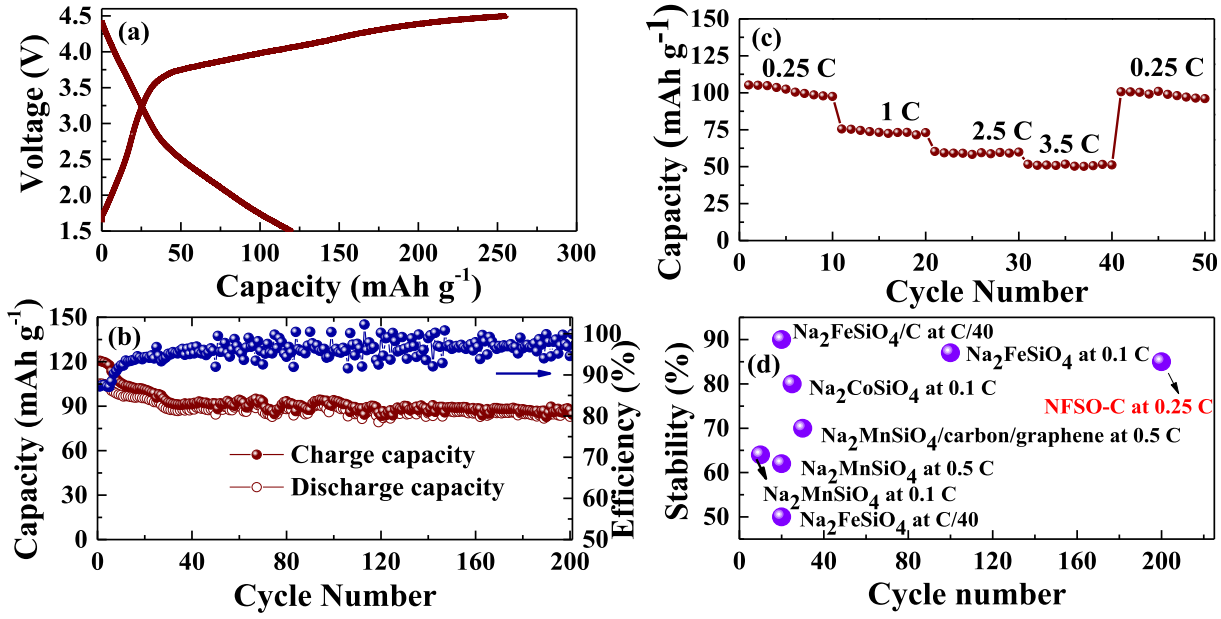

Fig. 3. (a) Initial C/DC curve of NFSO-C electrode recorded at 0.25 C within the 1.5 V - 4.5 V potential range. (b) Cycling performance of NFSO-C at 0.25 C (0.15 mA cm^{-2}) rate and (c) rate performance of NFSO-C at different current rates and (d) comparison of the cyclic stability of NFSO-C with other orthosilicates materials cycled at different current rates.

based methods (SG and HT).

The long-term cycling stability is a key factor for adopting any cathodes in practical applications. The cycling performance of NFSO-C at 0.25 C for 200 cycles is presented in Fig. 3b. The cell exhibits a discharge capacity of 105 mAh g^{-1} (after the activation step) at 0.25 C and maintains a capacity retention of ~85% after 200 cycles. The rate performance of the NFSO-C electrode at 0.25 C, 1 C, 2.5 C, and 3.5 C is presented in Fig. 3c. Discharge capacities of 105 mAh g^{-1}, 77 mAh g^{-1}, 62 mAh g^{-1}, and 55 mAh g^{-1} can be obtained from the half cell at 0.25 C, 1 C, 2.5 C, and 3.5 C, respectively. It is worth noting that the NFSO-C electrode delivers exceptional cyclic stability among sodium orthosilicates (NOS) between 1.5 V and 4.5 V at 0.25 C. The comparison of NOS cyclic stabilities at different cycle numbers is presented in Fig. 3d. It is clear that the half-cell containing NFSO-C cathode exceeds most of the cyclic stabilities of its counter parts. For instance, NMS with graphene (carbon content ~25%) shows a discharge capacity of 130 mAh g^{-1} and maintains 70% of its initial capacity value after 25 cycles [15]. Law et al. reported NMS/carbon with 64% of capacity retention at a rate of 0.1 C after 20 cycles. Recently, NFS with 87%

capacity retention at a rate of 0.1 C after 100 cycles was reported by Guan and his co-workers [25]. Nonetheless, the reports on NFSO with long-term cyclability at high current rate is scarce. As seen in Fig. 3d, most studies were stopped before 30 cycles at low current densities of 0.1 C or C/40. In the present work, we are reporting the long-term cycling ability of the NFSO-C cathode at different current rates for 150 cycles (Fig. 4a). As seen from Fig. 4a, the NFSO-C/Na^+ cell delivers discharge capacities of 75 mAh g^{-1}, 62 mAh g^{-1}, and 55 mAh g^{-1} at 1 C, 2.5 C, and 3.5 C and exhibits exceptional stability even after 150 cycles. The NFSO-C electrode is further C/DC at a rate of 3.5 C for 1000 cycles and the plot of capacity retention vs cycle number is presented in Fig. 4b. It is revealed that the NFSO-C electrode can maintain ~80% of its initial discharge capacity of 55 mAh g^{-1} after 1000 cycles at a rate of 3.5 C. To the best of our knowledge, the long-term cyclability achieved in the present work is the best one among the NOS at high current rates [15–17,20,21,25,36–38]. This appealing electrochemical cyclic performance at high current rate make NFSO-C electrode as a low cost and environmental friendly electrode material for next generation sodium ion batteries.

The excellent electrochemical behaviour of NFSO-C even at high currents can be attributed to the following reasons: (i) NFSO-C with ultrathin carbon-coating on the surface prevents the dissolution of active species into the electrolyte, which restricts unwanted side reactions and thus enhances the electrochemical performance [36]; (ii) the relatively large surface area of porous NFSO-C particles (as observed through SEM and TEM images) stores more electrolytes within its structure, increasing its performance during the high rate C/DC cycling processes. This flexible electrode helps to eliminate inherent mechanical stress at the high-rate cycling process and, thus, will enhance the electrochemical stability at the high current rate [15,29]; (iii) the ultrathin carbon-coating on NFSO-C surface is crucial for improving the conductive nature of the parent materials. The carbon on the surface ensures better contact between the particles and current collector, enabling smooth current flow on the surface and improved rate performance [24]; and, most importantly, (iv) NFSO-C without any impurities further confirms the improvement of electrochemical stability. Impurity phases have a great impact on the stability of cathode materials [16,24,25,28] The presence of impurities in the cathode material can participate in electrochemical reactions, leading to the formation of secondary phases during C/DC and affecting the cycling performance. It has been demonstrated that the metal orthosilicates prepared with impurity phases either exhibit low discharge capacities or severe capacity decay upon cycling even at low current rates [15–17,20,21,25,36]. Furthermore, the strong Si-O bond translates into very stable electrochemical and thermal properties, which are important for safety.

Electrochemical impedance spectroscopy (EIS) was employed to obtain information about the impact of particle size and carbon content on the electrochemical performance. Fig. 4c presents a typical Nyquist plot for the NFSO-C/Na^+ half-cell recorded before and after cycled at 3 C current rates for 1000 cycles within the frequency range of 200 kHz to 100 MHz. The EIS curves are fitted based on the equivalent circuit given in Fig. 4d. From the Nyquist plot, the first intersection point on the real axis in the high frequency region is associated to the solution resistance of the electrolyte (R_s). A semicircle is observed on the real axis at medium frequencies, corresponding to the kinetic control regime.[18] Furthermore, the semicircle develops moving across the Helmholtz plane, and is represented by the interfacial contact capacitance (C_c) and charge transfer resistance (R_{ct}). The values of R_{ct} calculated before and after cycles are about 120.32 Ω and 145.21 Ω, respectively, which is a ~25 Ω difference in charge transfer resistance before and after cycles. This low difference in resistance during C/DC is directly increased the current flow on the surface of the electrode, which facilitates the diffusing rate of the Na^+ ions toward the electrode even at high current rates [27]. Generally, higher resistance after deep C/DC cycles has a detrimental effect on ion diffusion at high current rates because the large polarization lowers the current flow and thus limits the electrochemical performance [10,27]. Nevertheless, in the present investigation, the lower difference in the R_{ct} value clearly demonstrates that the formation of a stable SEI layer film enhances the cycling stability [9,10]. This argument correlates well with the results obtained from the cycling performance presented in Figs. 3b and 4b. The improved conductivity of the electrode can also be attributed to the presence of uniform carbon coating on the surface and evenly distributed nanosized, primary NFSO-C particles. It is apparent that the phase pure high performance NFSO cathodes could be prepared using

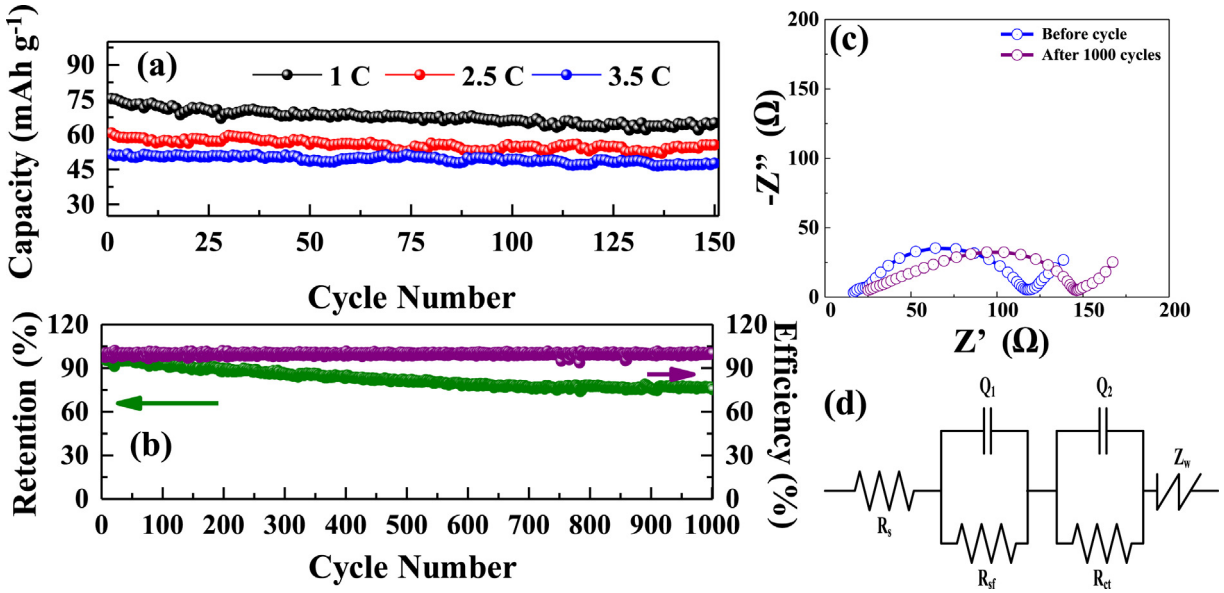

Fig. 4. (a) Cyclic performance of NFSO-C/Na^+ cell at different current rates and (b) long-term cyclic performance of NFSO-C/Na^+ cell at a rate of 3.5 C between 1.5 and 4.5 V for 1000 cycles. (c) EIS spectra of the NFSO-C/Na^+ cell recorded before and after 1000 cycles at 3.5 C rate and (d) equivalent circuit of the EIS spectrums.

solid-state method.

4. Conclusions

Carbon-coated Na_2FeSiO_4 powders without any impurities have been successfully synthesized using solid state methods with carboxylic acid as the chelating reagent as well as the carbon source. XRD and TEM images clearly show the absence of secondary phases and the presence of ultrathin uniform carbon layer on the Na_2FeSiO_4 particles, respectively. The best electrochemical performance is achieved from the half-cell containing carbon-coated Na_2FeSiO_4 electrode with superior capacity retention of 85%, at 0.25 C within the potential range of 1.5 V–4.5 V after 200 cycles. This cell also has superior cycling performance (80% retention after 1000 cycles) even at a rate of 3.5 C, owing to its high surface area and high purity. In addition, impedance results demonstrate the smallest charge-transfer resistance difference between before and after cycles, confirming its excellent structural stability even after long cyclic process. The impressive outcomes of this work can provide an economic way to synthesize highly stable, eco-friendly, Na_2FeSiO_4 particles in bulk for advanced sodium-ion storage applications.

Acknowledgment

This research was supported by the Natural Sciences and Engineering Research Council of Canada (NSERC). The TEM characterizations were conducted at the Canadian Center for Electron Microscopy (CCEM) at McMaster University.

References

[1] M. Armand, J.M. Tarascon, Building better batteries, Nature 451 (2008) 652–657.
[2] J. Yi, S. Guo, P. He, H. Zhou, Status and prospects of polymer electrolytes for solid-state Li-O2 (air) batteries, Energy Environ. Sci. 10 (2017) 860–884.
[3] M. Barghamadi, A. Kapoor, C. Wen, A review on Li-S batteries as a high efficiency rechargeable lithium battery, J. Electrochem. Soc. 160 (2013) A1256–A1263.
[4] M.D. Slater, D. Kim, E. Lee, C.S. Johnson, Sodium-ion batteries, Adv. Funct. Mater. 23 (2013) 947–958.
[5] M.S. Whittingham, Chemistry of intercalation compounds: metal guests in chalcogenide hosts, Prog. Solid State Chem. 12 (1978) 41–99.
[6] J.-P. Parant, R. Olazcuaga, M. Devalette, C. Fouassier, P. Hagenmuller, Sur quelques nouvelles phases de formule NaxMnO2 ($x \leq 1$), J. Solid State Chem. 3 (1971) 1–11.
[7] V. Palomares, P. Serras, I. Villaluenga, K.B. Hueso, J. Carretero-Gonzalez, T. Rojo, Na-ion batteries, recent advances and present challenges to become low cost energy storage systems, Energy Environ. Sci. 5 (2012) 5884–5901.
[8] V. Palomares, M. Casas-Cabanas, E. Castillo-Martinez, M.H. Han, T. Rojo, Update on Na-based battery materials. A growing research path, Energy Environ. Sci. 6 (2013) 2312–2337.
[9] H.V. Ramasamy, K. Kaliyappan, R. Thangavel, V. Aravindan, K. Kang, D.U. Kim, Y. Park, X. Sun, Y.-S. Lee, Cu-doped P2-Na0.5Ni0.33Mn0.67O2 encapsulated with MgO as a novel high voltage cathode with enhanced Na-storage properties, J. Mater. Chem. A 5 (2017) 8408–8415.
[10] K. Kaliyappan, J. Liu, A. Lushington, R. Li, X. Sun, Highly stable Na2/3(Mn0.54Ni0.13Co0.13)O2 cathode modified by atomic layer deposition for sodium-ion batteries, ChemSusChem 8 (2015) 2537–2543.
[11] H. Wang, B. Yang, X.-Z. Liao, J. Xu, D. Yang, Y.-S. He, Z.-F. Ma, Electrochemical properties of P2-Na2/3[Ni1/3Mn2/3]O2 cathode material for sodium ion batteries when cycled in different voltage ranges, Electrochim. Acta 113 (2013) 200–204.
[12] R. Thangavel, K. Kaliyappan, K. Kang, X. Sun, Y.-S. Lee, Going beyond lithium hybrid capacitors: proposing a new high-performing sodium hybrid capacitor system for next-generation hybrid vehicles made with bio-inspired activated carbon, Adv. Energy Mater. 6 (2016). 1502199-n/a.
[13] S.-M. Oh, S.-T. Myung, J. Hassoun, B. Scrosati, Y.-K. Sun, Reversible NaFePO4 electrode for sodium secondary batteries, Electrochem. Commun. 22 (2012) 149–152.
[14] J. Kim, D.-H. Seo, H. Kim, I. Park, J.-K. Yoo, S.-K. Jung, Y.-U. Park, W.A. Goddard Iii, K. Kang, Unexpected discovery of low-cost maricite NaFePO4 as a high-performance electrode for Na-ion batteries, Energy Environ. Sci. 8 (2015) 540–545.
[15] H. Zhu, J. Wang, X. Liu, X. Zhu, Facile preparation of a Na2MnSiO4/C/graphene composite as a high performance cathode for sodium ion batteries, RSC Adv. 7 (2017) 14145–14151.
[16] Y. Kee, N. Dimov, A. Staykov, S. Okada, Investigation of metastable Na2FeSiO4 as a cathode material for Na-ion secondary battery, Mater. Chem. Phys. 171 (2016) 45–49.
[17] X. Zhao, S. Wu, X. Lv, M.C. Nguyen, C.-Z. Wang, Z. Lin, Z.-Z. Zhu, K.-M. Ho, Exploration of tetrahedral structures in silicate cathodes using a motif-network scheme, Sci. Rep. 5 (2015) 15555.
[18] Y. Zhang, H. Yu, H. Zhou, Two-electron migration orthosilicate cathode materials for Na-ion batteries, J. Mater. Chem. A 2 (2014) 11574–11577.
[19] Z. Ye, X. Zhao, S. Li, S. Wu, P. Wu, M.C. Nguyen, J. Guo, J. Mi, Z. Gong, Z.-Z. Zhu, Y. Yang, C.-Z. Wang, K.-M. Ho, Robust diamond-like Fe-Si network in the zero-strain NaxFeSiO4 cathode, Electrochim. Acta 212 (2016) 934–940.
[20] P. Wu, S.Q. Wu, X. Lv, X. Zhao, Z. Ye, Z. Lin, C.Z. Wang, K.M. Ho, Fe-Si networks in Na2FeSiO4 cathode materials, Phys. Chem. Chem. Phys. 18 (2016) 23916–23922.
[21] S. Li, J. Guo, Z. Ye, X. Zhao, S. Wu, J.-X. Mi, C.-Z. Wang, Z. Gong, M.J. McDonald, Z. Zhu, K.-M. Ho, Y. Yang, Zero-Strain Na2FeSiO4 as novel cathode material for sodium-ion batteries, ACS Appl. Mater. Interfaces 8 (2016) 17233–17238.
[22] F. Bianchini, H. Fjellvag, P. Vajeeston, First-principles study of the structural stability and electrochemical properties of Na2MSiO4 (M = Mn, Fe, Co and Ni) polymorphs, Phys. Chem. Chem. Phys. 19 (2017) 14462–14470.
[23] H. Duncan, A. Kondamreddy, P.H.J. Mercier, Y. Le Page, Y. Abu-Lebdeh, M. Couillard, P.S. Whitfield, I.J. Davidson, Novel pn polymorph for Li2MnSiO4 and its electrochemical activity as a cathode material in Li-Ion batteries, Chem. Mater. 23 (2011) 5446–5456.
[24] K. Karthikeyan, S. Amaresh, G.W. Lee, V. Aravindan, H. Kim, K.S. Kang, W.S. Kim, Y.S. Lee, Electrochemical performance of cobalt free, Li1.2(Mn0.32Ni0.32Fe0.16)O2 cathodes for lithium batteries, Electrochim. Acta 68 (2012) 246–253.
[25] W. Guan, B. Pan, P. Zhou, J.-X. Mi, D. Zhang, J. Xu, Y. Jiang, A High Capacity, Good Safety and Low Cost Na2FeSiO4-based Cathode for Rechargeable Sodium-ion Battery, ACS Applied Materials & Interfaces, 2017.
[26] K. Karthikeyan, V. Aravindan, S.B. Lee, I.C. Jang, H.H. Lim, G.J. Park, M. Yoshio, Y.S. Lee, Electrochemical performance of carbon-coated lithium manganese silicate for asymmetric hybrid supercapacitors, J. Power Sources 195 (2010) 3761–3764.
[27] K. Karthikeyan, V. Aravindan, S.B. Lee, I.C. Jang, H.H. Lim, G.J. Park, M. Yoshio, Y.S. Lee, A novel asymmetric hybrid supercapacitor based on Li2FeSiO4 and activated carbon electrodes, J. Alloys Compd. 504 (2010) 224–227.
[28] Y.-s. Lee, Y.-K. Sun, K.-S. Nahm, Synthesis of spinel LiMn2O4 cathode material prepared by an adipic acid-assisted sol–gel method for lithium secondary batteries, Solid State Ionics 109 (1998) 285–294.
[29] K. Karthikeyan, S. Amaresh, V. Aravindan, W.S. Kim, K.W. Nam, X.Q. Yang, Y.S. Lee, Li(Mn1/3Ni1/3Fe1/3)O2–Polyaniline hybrids as cathode active material with ultra-fast charge–discharge capability for lithium batteries, J. Power Sources 232 (2013) 240–245.
[30] X. Huang, Y. You, Y. Ren, H. Wang, Y. Chen, X. Ding, B. Liu, S. Zhou, F. Chu, Spray drying-assisted synthesis of hollow spherical Li2FeSiO4/C particles with high performance for Li-ion batteries, Solid State Ionics 278 (2015) 203–208.
[31] K. Karthikeyan, S. Amaresh, S.N. Lee, X. Sun, V. Aravindan, Y.-G. Lee, Y.S. Lee, Construction of high-energy-density supercapacitors from pine-cone-derived high-surface-area carbons, ChemSusChem 7 (2014) 1435–1442.
[32] K. Karthikeyan, D. Kalpana, S. Amaresh, Y.S. Lee, Microwave synthesis of graphene/magnetite composite electrode material for symmetric supercapacitor with superior rate performance, RSC Adv. 2 (2012) 12322–12328.
[33] Q. Qu, S. Yang, X. Feng, 2D sandwich-like sheets of iron oxide grown on graphene as high energy anode material for supercapacitors, Adv. Mater. 23 (2011) 5574–5580.
[34] K. Wang, W. Ren, J. Yang, R. Tan, Y. Liu, F. Pan, Depolarization effects of Li2FeSiO4 nanocrystals wrapped in different conductive carbon networks as cathodes for high performance lithium-ion batteries, RSC Adv. 6 (2016) 47723–47729.
[35] P. Simon, Y. Gogotsi, Materials for electrochemical capacitors, Nat. Mater. 7 (2008) 845–854.
[36] J.C. Treacher, S.M. Wood, M.S. Islam, E. Kendrick, Na2CoSiO4 as a cathode material for sodium-ion batteries: structure, electrochemistry and diffusion pathways, Phys. Chem. Chem. Phys. 18 (2016) 32744–32752.
[37] M. Law, V. Ramar, P. Balaya, Na2MnSiO4 as an attractive high capacity cathode material for sodium-ion battery, J. Power Sources 359 (2017) 277–284.
[38] C.-Y. Chen, K. Matsumoto, T. Nohira, R. Hagiwara, Na2MnSiO4 as a positive electrode material for sodium secondary batteries using an ionic liquid electrolyte, Electrochem. Commun. 45 (2014) 63–66.